Structure of a Ring-Containing Fluoropolymer

Soo-Young Park, S. N. Chvalun,† and J. Blackwell*

Department of Macromolecular Science, Case Western Reserve University, Cleveland, Ohio 44106-7202

Received May 22, 1997; Revised Manuscript Received August 18, 1997[⊗]

ABSTRACT: The structure of a ring-containing fluoropolymer poly(1,2-difluoromethylene-1,2,3,3-tetrafluoro-4,4-dihydrofuran) has been investigated by X-ray methods. Pressed films are more than 60% crystalline, and small-angle X-ray data show that these contain lamellae oriented with their long axes parallel to the surface. The wide-angle X-ray data show that the chains are perpendicular to the film surface and have an axial repeat of 9.62 Å, probably containing two monomers (an axial advance of 4.81 Å per monomer). Molecular mechanics modeling indicates that the most likely structure contains syndiotactic chains in which the monomers have the *threo* configuration: such chains are ribbonlike, with an axial advance of ∼4.8 Å, in good agreement with the observed repeat. In contrast, the preferred conformation for the isotactic chain of *threo* monomers is a nonintegral helix with close to five monomers per turn and an axial advance of ∼4.1 Å/monomer, which is not compatible with the X-ray data. Chains of monomers in the higher energy *erythro* configuration have monomer repeats in the region of 3.9−4.2 Å and appear unlikely. Thus, the results suggest that the high degree of crystallinity is due to a highly syndiotactic, probably blocky microstructure for the polymer.

Introduction

Fluorine-containing polymers are known for their excellent dielectric properties and weatherability, low coefficient of friction, and chemical inertness but are generally resistant to acids and bases and insoluble in common organic solvents.[1−3] Notable exceptions with regard to insolubility are ring-containing polymers such as Teflon-AF (DuPont)[4,5] and Cytop (Asahi Glass)[6,7]

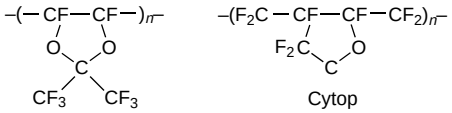

which have limited solubility in commercially available perfluorinated ethers such as Fluorinert FC-75. These materials exhibit the characteristic electrical and thermal properties and the chemical resistance of fluoropolymers and also have high optical clarity and excellent physical properties below their glass transition temperatures. They may be solution-cast as clear films or melt-processed in a variety of forms. However, in contrast to poly(tetrafluoroethylene), these polymers are amorphous.

Recently, a new ring-containing fluoropolymer has been reported by Yang et al.[8] It was prepared by cyclopolymerization of a partially fluorinated diene ether (1,1-dihydro-2,2,3,4,4-pentafluoro-3-butenyl trifluorovinyl ether) using a mixture of bis(perfluoropropionyl) peroxide and bis(4-*tert*-butylcyclohexylperoxy) dicarbonate as the initiator:

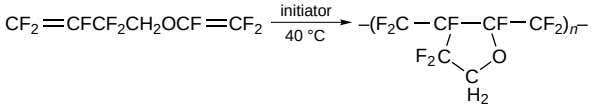

The resultant polymer is poly(1,2-difluoromethylene-1,2,3,3-tetrafluoro-4,4-dihydrofuran) (PDTE). The presence of the two ring hydrogens increases the polarity compared to that of the fully fluorinated analog, such that this polymer is soluble in polar aprotic solvents such as dimethylformamide (DMF), tetrahydrofuran (THF), acetone, and acetonitrile. In addition, this polymer is crystalline, even though no efforts had been made to control the tacticity. The glass transition and melting temperatures are 127 and 347 °C, respectively.

It is very interesting as to why this polymer is crystalline in contrast to Cytop, which has the same chemical structure except for the additional ring fluorines. The microstructure is unknown at this point, but it is possible that the presence of the hydrogen may lead to a preferred tacticity, making crystallization possible. The presence of the ring hydrogens may allow for easier interdigitation of the rings on adjacent chains, and there may also be the possibility of favorable interchain dipole−dipole interaction. We have investigated the crystal structure of PDTE in order to throw light on these problems.

Experimental Section

The specimen of PDTE was generously provided by Drs. Zhen-yu Yang, Andrew E. Feiring, and Bruce E. Smart (DuPont) and had been prepared in the manner described in ref 8, which yielded a polymer with $M_n = 190\,000$ and $M_w = 404\,000$ based on GPC data. A film (0.5 mm thick) of this material prepared by casting from DMF solution was brittle and could not be drawn. Orientation was achieved by compression of the film to half its original thickness by application of a pressure of 1000 kg/mm^2 at 250 °C. The density was measured by flotation in tetrachloroethylene and 1,2-dibromoethane, which are miscible nonsolvents.

The wide-angle X-ray scattering of the original cast film was recorded as a $\theta/2\theta$ scan on a Philips PN 3550/10 diffractometer operating in the transmission mode, using Ni-filtered Cu Kα radiation. The degree of crystallinity was determined by separation of these data into crystalline and amorphous components, after subtraction of the background scattering. The apparent crystal size was measured from the width at half-height of the Bragg peak at $d = 6.07$ Å using the Scherrer equation. Wide- and small-angle X-ray patterns of the pressed films were recorded on Kodak Direct Exposure film, with the beam perpendicular and parallel to the surface of a film. For the wide-angle experiments we used a Searle toroidal focusing

* To whom correspondence should be addressed.
† Present address: Karpov Institute of Physical Chemistry, ul. Vorontzovo Pole 10, 103064 Moscow, Russia.
⊗ Abstract published in *Advance ACS Abstracts,* October 1, 1997.

S0024-9297(97)00717-1 CCC: $14.00

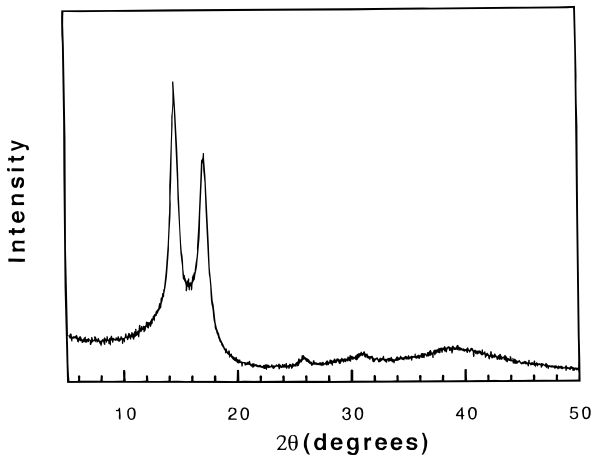

Figure 1. $\theta/2\theta$ diffractometer scan of a solution-cast film of PDTE.

camera, and the specimen-to-film distance was calibrated with calcium fluoride. The small-angle X-ray patterns were recorded using pinhole collimation.

Energy minimization of molecular models was performed with the SYBYL software package (Tripos Inc.). The polymer backbone is defined by four torsional angles, ξ, ζ, ϕ_1, and ψ, and the conformation of the ring by ϕ_1–ϕ_5:

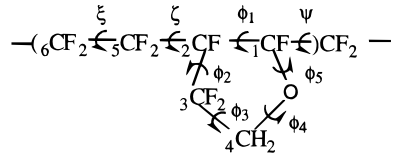

Zeros for these torsion angles are for the *cis* positions for the carbon or oxygen atoms, and positive angles correspond to anticlockwise rotations. The force field was modified by incorporating the preferred bond lengths, bond angles, van der Waals radii, and energy parameters used by Holt et al.,[9] to model the structure of poly(tetrafluoroethylene). The potential energies were computed as the sum of the contribution due to van der Waals and electrostatic forces, distortions of the bond lengths, bond angles, and torsional angles, and the effects of out-of-plane bending. Energy minimizations were terminated when the energy difference between successive cycles was less than 0.01 kcal/mol.

Results and Discussion

X-ray Diffraction. Figure 1 shows a $\theta/2\theta$ wide-angle diffractometer scan for the cast film recorded in the transmission mode, with the film perpendicular to the beam at $\theta = 0°$. Division of the scattering into crystalline and amorphous contributions assigns at least 60% of the total to the crystalline regions. The absolute percentage crystallinity is difficult to assess because of problems in predicting the amorphous halo, but it is clear that PDTE is highly crystalline. A crystallite width of 117 ± 10 Å is derived from the first Bragg peak at $d = 6.07$ Å, which is also relatively large, consistent with the high degree of crystallinity.

The small- and wide-angle X-ray scattering patterns were recorded with the beam parallel and perpendicular to the film surface, as shown in Figure 2. When the beam was parallel to the film surface, we observed a single maximum in the small-angle region at $d = 110 \pm 10$ Å (Figure 2a), which is inclined along the direction perpendicular to the film surface. There was only diffuse scattering in the small-angle region when the beam was perpendicular to the film surface (Figure 2b). The likely interpretation of these data is that the specimen contains crystalline, chain-folded lamellae which are stacked with their long axes preferentially parallel to the film surface, as a result of the applied compression.

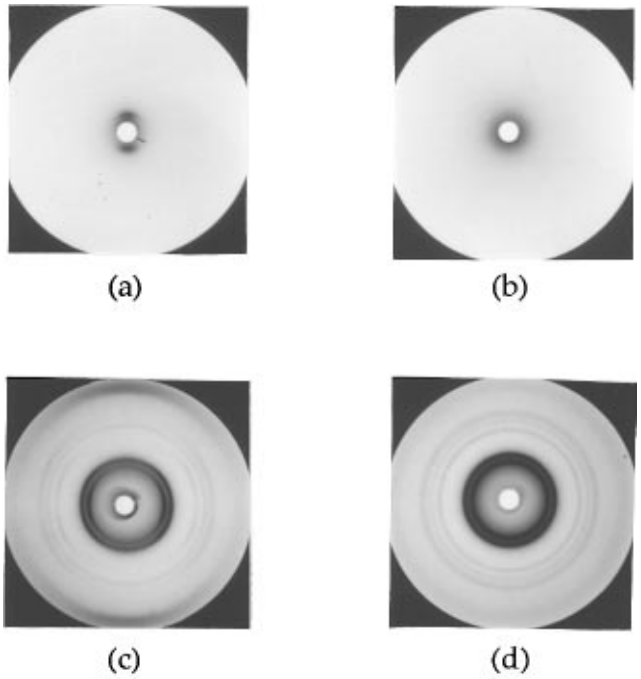

Figure 2. Wide- and small-angle X-ray patterns of a pressed film of PDTE: (a) small-angle beam parallel to the film surface; (b) small-angle beam perpendicular to the film surface; (c) wide-angle beam parallel to film surface; (d) wide-angle beam perpendicular to the film surface. The vertical direction in parts a and c is perpendicular to the film surface.

Table 1. Observed *d*-Spacings and *R*, *Z* Reciprocal Space Coordinates for Wide-Angle Bragg Reflections with the Beam Parallel to the Film Surface.

no.	d (Å)	Z (Å^{-1})	R (Å^{-1})	$1/R$(Å)
1	6.07 ± 0.03	0	0.165	6.07
2	5.18 ± 0.01	0.104	0.163	6.15
3	4.81 ± 0.03	0.208	0	meridional
4	3.75 ± 0.01	0.208	0.167	6.00
5	3.50 ± 0.01	0.104	0.266	3.76
6	2.92 ± 0.02	0.104	0.326	3.06
		0.208	0.272	3.68
7	2.59 ± 0.01	0	0.386	2.59
		0.104	0.372	2.69
		0.208	0.325	3.07
		0.312	0.228	4.39
8	2.33 ± 0.1	0.429	0	meridional

The wide-angle data recorded with the beam perpendicular to the film surface are shown in Figure 2d and consist of eight isotropic rings with *d*-spacings as listed in Table 1. These *d*-spacings are similar to those for the peaks in the diffractometer scan (Figure 1), but there are some differences in intensity resulting from the preferred orientation. The data indicate complete rotational disorder of the crystallites about an axis perpendicular to the film surface. In the case where the beam was parallel to the film surface (Figure 2c), these rings are broken into arcs. A schematic of the latter data is presented in Figure 3, where the Bragg reflections are numbered for reference in the text. The observed *R*, *Z* reciprocal space coordinates for the reflections are given in Table 1 and are plotted in Figure 3 (inset). The *R* and *Z* axes are parallel and perpendicular to the film surface, respectively, and will be referred to as the equator and meridional, respectively.

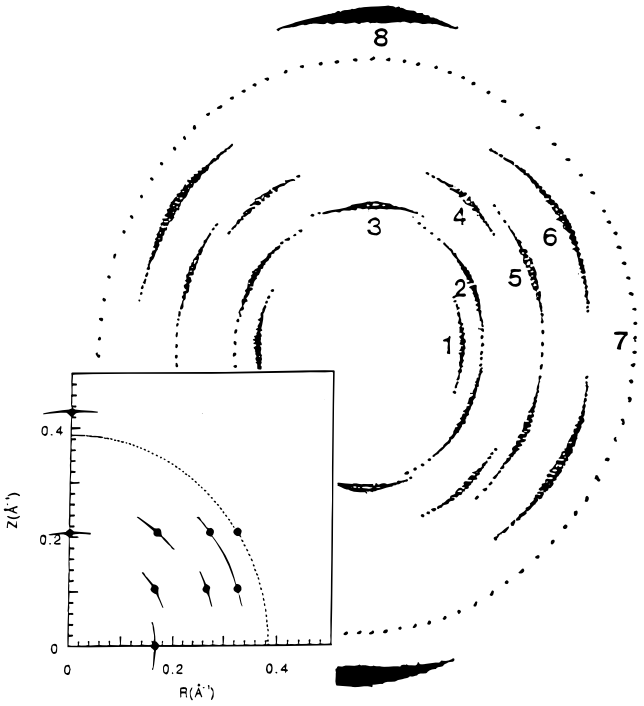

Figure 3. Schematic of the wide-angle X-ray pattern recorded with the X-ray beam parallel to the film surface (Figure 2c). Inset: positions of the Bragg reflections plotted in R, Z reciprocal space coordinates ($Å^{-1}$).

Two reflections (nos. 3 and 8) occur along the meridian at $d = 4.81$ and 2.33 Å; the latter is broad, and its d-spacing is within experimental error of the second order of reflection no. 3. One reflection (no. 1) occurs on the equator at $d = 6.07$ Å. Of the off-axis reflections, that at $d = 3.75$ Å (no. 4) has the same Z coordinate as the meridional reflection at $d = 4.81$ Å (no. 3); those at $d = 5.18$ and 3.50 Å (nos. 2 and 5) have the same Z coordinate, which is half that of reflections 3 and 4. It can also be seen that reflections 1, 2, and 4 have the same R coordinate. Thus the data in Figures 2c and 3 have the appearance of a fiber diagram consisting of the equator and layer lines 1, 2, and 4 for a repeat of $c = 9.6$ Å, with a distinct row line at $R = 1/6.07$ $Å^{-1}$. Reflection no. 6 at $d = 2.92$ Å is more arced than reflections 1−5 and 7 and straddles layer lines 1 and 2. A component at this d-spacing on the second layer line would have the same R coordinate as reflection no. 5; a component on the first layer line would have $R = 2/6.07$ $Å^{-1}$; i.e., it would be at the second order of the row line formed by reflections 1, 2, and 4. The reflection at $d = 2.59$ Å (no. 7) is an isotropic ring, but a component on the second layer line would also have $R = 2/6.07$ $Å^{-1}$.

The existence of both layer lines and row lines suggests at least monoclinic symmetry for the polymer unit cell with the chains perpendicular to the film surfaces. Thus, reflections 3 and 8 are assigned 002 and 004 indices, and the absence of odd orders suggests that the chain conformation has two structural units repeating in $c = 9.6$ Å. A unit cell cannot be proposed on the data available, but basing a and b on the spacings of the first two row lines, an orthorhombic unit cell with dimensions $a = 6.07$ Å, $b = 3.76$ Å, and $c = 9.62$ Å containing two monomer units would have a density of 2.19 $g{\cdot}mL^{-1}$ compared to the observed density of 2.00 $g{\cdot}mL^{-1}$ for the semicrystalline specimen. (Note that the b dimension would need to be doubled ($b = 7.52$ Å) in order to accommodate the present fluoropolymer chemistry, so the most likely structure has a unit cell containing dimer units of two chains.) The observed and calculated densities are reasonably close, and the match would improve if we adopted monoclinic geometry with $\gamma \neq 90°$.

Model Building. There are four possible configurations for the ring as a result of the asymmetric centers at C_1 and C_2: D-*threo*, L-*threo*, D-*erythro*, and L-*erythro*, as shown schematically in Figure 4. In the *threo* configurations, the CF_2 groups at C_1 and C_2 are *trans*; i.e., they point to opposite sides of the average plane containing the ring atoms, whereas these substituents are *cis* in the *erythro* configurations. The minimum-energy conformations for the D-*threo* and L-*threo* monomers are given in Table 2 (conformation I in each case). The equivalent conformations for the L-configurations are mirror images with the same energies. As expected, the rings are puckered, with C_3 and C_4 out of the $O-C_1-C_2$ plane. The minimum energies for the *erythro* configurations are 1.6 kcal/mol higher than those for the *threo* configurations, due to the *cis* disposition of the substituents. Exploration of the conformational space of the monomer shows that three additional minimum-energy conformations exist for each configuration. The $\phi_1-\phi_5$ angles and the potential energies for these conformations for the D-*threo* and D-*erythro* configurations are also given in Table 2.

To consider the backbone conformation, we constructed all possible combinations of *threo* and *erythro* configurations, syndio- and isotactic sequences, and head-to-tail, head-to-head, and tail-to-tail combinations. The starting models had the rings in the lowest energy conformation I in each case. The minimum-energy conformations for the six possible *all-threo* dimers had the energies and torsion angles listed in Table 3. In all cases ξ, ζ, and ψ are in the region of 180°(*trans*). The deviations from *trans* occur primarily because of the van der Waals interactions between the fluorine atoms. These interactions are similar to those that occur in poly(tetrafluoroethylene), which lead to the 13_6 conformation rather than the *all-trans* 2_1 conformation seen for polyethylene.[9,10]

Examination of the *threo* disyndiotactic linkages shows that the CF_2-CF_2 spacer units in the head-to-head and tail-to-tail linkages are approximately centrosymmetric. Requiring them to be exactly so has a negligible effect on the potential energy and leads to a straight-chain conformation for the head-to-head/tail-to-tail polymer, with a repeat of 9.54 Å (4.77 Å advance per monomer), which is close to the dimension $c = 9.62$ Å proposed above based on the X-ray data. This conformation is shown in Figure 5a; note that successive monomers are D and L. A model for the disyndiotactic head-to-tail polymer constructed using the minimum-energy conformation for the dimer leads to a somewhat nonlinear chain, but this can be constrained to be linear with only a small rise in potential energy. There are many ways of achieving this linearity, by changing the torsion angles in both the spacer and the ring: the actual structure would probably be determined by packing considerations. It is clear, however, that the conformations and fiber repeats of the disyndiotactic head-to-tail and head-to-head/tail to tail polymers should be very similar to each other and to those of a syndiotactic chain with random head-to-tail/head-to-head linkages, with an axial advance of ~4.8 Å per monomer.

Figure 5b shows the conformation for the *threo* diisotactic chain with head-to-tail linkages constructed

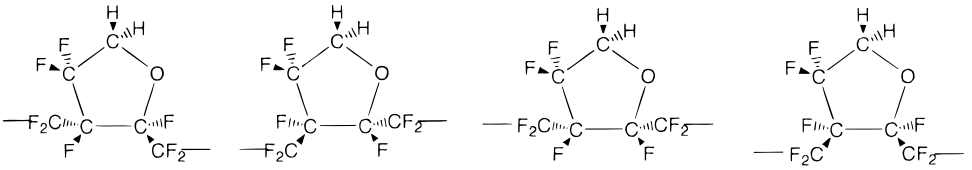

Figure 4. Schematics for the four possible chemical configurations for the tetrafluorodihydrofuranyl ring: D-*threo*, L-*threo*, D-*erythro*, and L-*erythro*.

Table 2. Torsional Angles (deg) for the Minimum-Energy Conformations of the Tetrafluorodihydrofuran Ring

	ϕ_1 (ϕ_1')	ϕ_2	ϕ_3	ϕ_4	ϕ_5	energy (kcal/mol)
			D-*threo*			
I	11.6 (−111.0)	15.2	−37.3	47.7	−38.0	7.3
II	45.7 (−76.0)	−27.1	0.8	30.3	−48.8	9.3
III	−29.4 (−153.0)	8.5	14.8	−36.2	42.2	8.2
IV	6.6 (−113.0)	−29.4	43.7	−42	22.4	9.6
			D-*erythro*			
I	−42.4 (−53.2)	23.2	2.2	−31.0	47.5	8.9
II	38.5 (42.0)	−20.1	−4.6	31.8	−44.6	13.6
III	17.3 (21.0)	−36.7	45.9	−36.8	12.2	14.8
IV[a]	−3.5 (−10.0)	26.8	−42.5	42.6	−24.9	15.9

[a] Conformation IV for D-*erythro* is at an inflection rather than an energy minimum. $\phi_1 = O-C_1-C_2-C_3$, $\phi_2 = C_1-C_2-C_3-C_4$, $\phi_3 = C_2-C_3-C_4-O$, $\phi_4 = C_3-C_4-O-C_1$, $\phi_5 = C_4-O-C_1-C_2$. The backbone torsion angle $\phi_1' = C_5-C_2-C_1-C_6$ is given in parentheses.

Table 3. Backbone Torsion Angles for the Minimum-Energy Conformation of the Six Possible Di-*threo* Units

	torsional angle (deg)					energy
tacticity[a]	ϕ_1	ζ	ξ	ψ	ϕ_1	(kcal/mol)
			threo Disyndiotactic			
H−T	−111	163	161	173	111	20.1
H−H	−111	161	177	199	111	28.7
T−T	−111	180	183	182	111	15.1
			threo Diisotactic			
H−T	−111	164	157	174	−111	16.4
H−H	−111	161	167	161	−111	22.5
T−T	−111	174	166	174	−111	13.2

[a] H−H: head-to-head. H−T: head-to-tail. T−T: tail-to-tail.

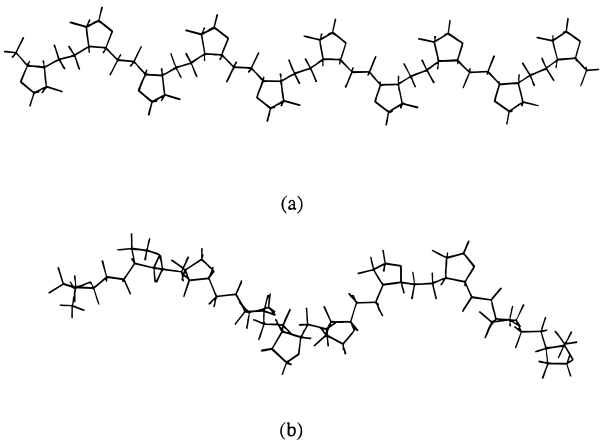

Figure 5. Minimum-energy conformations of PDTE chains: (a) syndiotactic head-to-head/tail-to-tail; (b) isotactic head-to-tail polymer chains.

using the torsion angles in Table 2. The chain is helical with close to five monomers per turn and a monomer advance of 4.05 Å. The head-to-head/tail-to-tail polymer has a similar conformation, as would a random head-to-tai/head-to-head option. Thus, for the *threo* diisotactic structures, we would expect to observe meridional intensity in the region of $d = 4.1$ Å, whereas the observed reflections are at $d = 4.81$ and 2.33 Å. This difference is well beyond experimental error and effectively rules out these structures.

Polymer structures containing *erythro* configurations are probably unlikely to be formed during synthesis, since these monomers have much higher energies than the equivalent *threo* configurations. When we construct the *erythro* disyndio- and diisotactic structures equivalent to the six *threo* structures considered above, the minimum-energy conformations are contracted compared to the equivalent *threo* structures: the monomer advances are ∼3.9 Å for diisotactic and ∼4.3 Å for disyndiotactic. In addition, their energies are also much higher: 80−120 kcal/mol of dimer.

Thus, the X-ray data favor a *threo* disyndiotactic structure. Distortion of a *threo* diisotactic polymer chain to have a conformation compatible with the observed repeat would involve a large rise in the potential energy. (For the D-configuration this would require a ϕ_1' torsion angle of about −111°, and none of the four minimum-energy conformations in Table 2 have ϕ_1' close to this value.) Hence, it is difficult to see many isotactic linkages being incorporated as defects in crystallites composed of predominantly *threo* syndiotactic chains. Likewise, the presence of *erythro* configurations would also represent major defects incompatible with crystallinity. Consequently, the very high degree of crystallinity points to the existence of long blocks of syndiotactic sequences of *threo* monomers. The structure of this polymer contrasts with that of Cytop, which is amorphous, and the simplest explanation for this is that the presence of the hydrogen at C_4 leads to a high preference for a syndiotactic addition during the polymerization reaction.

In the absence of a more definite unit cell, the chain packing cannot be determined. At this point it appears that both head-to-tail and head-to-head/tail-to-tail *all-threo* options could be accommodated. Even so, electrostatic interactions may occur in PDTE that are not possible in the fully fluorinated Cytop, which may further enhance the crystallinity. The possible existence of hydrogen bonding in lightly hydrogenated fluoropolymers has been discussed previously.[11] It has been suggested that polymers containing $-CF_2CH_2OCF_2-$ units have especially strong hydrogen-bonding ability, based on NMR chemical shifts observed for related small molecules.[12] It is also possible that the presence of large fluorine atoms at C_4 would inhibit crystalline packing even for a highly tactic polymer. However, better quality X-ray data would be necessary to investigate these possibilities.

Conclusions

Pressed films of the ring-containing fluoropolymer poly(1,2-difluoromethylene-1,2,3,3-tetrafluoro-4,4-dihy-

drofuran) are highly crystalline and contain lamellae that are oriented with their long axes parallel to the film surface. The wide-angle X-ray data recorded with the beam parallel to the film surface contain both layer lines and row lines, pointing to a crystal structure with at least monoclinic symmetry, in which the chain axes are perpendicular to the film surface. The layer line spacings define the repeat along the chain axis direction as $c = 9.62$ Å, probably containing two monomer units.

Molecular modeling points to a ribbonlike conformation for a syndiotactic polymer chain composed of alternating D- and L-*threo* monomers in a repeat of $c = \sim 9.5$ Å (~4.8 Å/monomer). This repeat is largely independent of the choice of head-to-tail, head-to-head, or tail-to-tail linkage and is in very good agreement with the observed X-ray data. In contrast, the minimum-energy conformations for the isotactic polymer composed of *threo* monomers are helices with approximately five monomers per turn and an axial advance per monomer of ~4.1 Å, which is inconsistent with the observed X-ray data. The structures composed of *erythro* monomers also have short axial repeats (3.9−4.3 Å/monomer) and have much higher potential energies. Random copolymerization of monomers with different configurations is unlikely to lead to a crystalline structure. Thus, PDTE probably has a highly syndiotactic/*all-threo* microstructure in order to account for the high degree of crystallinity (at least 60%).

Acknowledgment. We thank Drs. Zhen-yu Yang, Andrew E. Feiring, and Bruce E. Smart of DuPont Central Research, Wilmington, DE, for providing the specimen of PDTE and for very helpful discussion.

References and Notes

(1) Wall, L. A. *Fluoropolymers*; Wiley: New York, 1972; Vol. XXV.
(2) Schmiegel, W. W. *Chemistry of Organic Fluorine Compounds II. ACS Monogr.* **1995**, *187*, 1101−1118.
(3) Feiring, A. E. In *Organofluorine Chemistry, Principles and Commercial Applications*; Banks, R. E., Smart, B. E., Tatlow, J. C., Eds.; Plenum: New York, 1994; pp 339−72.
(4) Resnick, R. R. *Polym. Prepr. (Am. Chem. Soc., Div. Polym. Chem.)* **1990**, *31*, 312.
(5) Korinek, P. M. *Macromol. Symp.* **1994**, *82*, 61.
(6) Nakamura, N.; Kawasaki, T.; Unoki, M.; Sugiyama, N.; Kaneko, I.; Kojima, G. *Prepr. 1st Pac. Polym. Conf.* **1989**, 369.
(7) Yamabe, M.; Matsuo, M.; Miyake, H. *Plast. Eng.* **1997**, *40*, 429.
(8) Yang, Z.-Y.; Feiring, A. E.; Smart, B. E. *J. Am. Chem. Soc.* **1994**, *116*, 4135.
(9) Holt, D. B.; Farmer, B. L.; Macturk, K. S.; Eby, R. K. *Polymer* **1996**, *37*, 1847.
(10) Bunn, C. W.; Howells E. R. *Nature* **1954**, *174*, 549.
(11) Hung, M. H.; Farnham, W. B.; Feiring, A. E.; Rozen, S. *J. Am. Chem. Soc.* **1993**, *115*, 8954.
(12) Feiring, A. E.; Wonchoba, E. R. *J. Org. Chem.* **1992**, *57*, 7014.

MA970717F